

RSC Advances



This is an *Accepted Manuscript*, which has been through the Royal Society of Chemistry peer review process and has been accepted for publication.

Accepted Manuscripts are published online shortly after acceptance, before technical editing, formatting and proof reading. Using this free service, authors can make their results available to the community, in citable form, before we publish the edited article. This *Accepted Manuscript* will be replaced by the edited, formatted and paginated article as soon as this is available.

You can find more information about *Accepted Manuscripts* in the [Information for Authors](#).

Please note that technical editing may introduce minor changes to the text and/or graphics, which may alter content. The journal's standard [Terms & Conditions](#) and the [Ethical guidelines](#) still apply. In no event shall the Royal Society of Chemistry be held responsible for any errors or omissions in this *Accepted Manuscript* or any consequences arising from the use of any information it contains.



Journal Name

ARTICLE

Shear-force-dominated Dual-Drive Planetary Ball milling for Scalable Production of Graphene and Its Electrocatalytic Application with Pd nanostructures

Received 00th January 20xx,
Accepted 00th January 20xx

DOI: 10.1039/x0xx00000x

www.rsc.org/

G. Rajendra Kumar^{a,b}, K. Jayasankar^{*a}, Sushanta K. Das^a, Tapan Dash^a, Ajit Dash^a, Bikash Kumar Jana^a, B.K.Mishra^a

The exceptional properties of graphene-based derivatives have governed the numerous research fields in recent years. The scaled up, and reliable production of high-quality graphene is still a challenging task. This work elucidates the efficient and low-cost approach for mass production of high-quality graphene (50g scale batch) through dual-drive planetary ball milling of graphite with the dicarboxylic acid. The dimensional changes of graphite derived from the diffraction pattern of (002) plane at different milling hours and the unique signature of the graphene noticed in Raman spectroscopy. Transmission electron microscopy clearly envisioned the existence of single and bilayer graphene sheets. The non-destructive exfoliation evidenced by the surface binding states of C 1s core level spectra. The as-synthesized graphene utilized as the catalytic support for formic acid fuel cell applications. The graphene supported palladium nanocomposites prepared, and the electrocatalytic activity towards the formic acid oxidation explored. The cyclic voltammetry of graphene-palladium nanocomposite reveals the onset potential for formic acid oxidation at -0.1 V with prominent oxidation peak at 0.263 V.

1. Introduction

The discovery of new material offers the most exciting and fruitful periods of scientific and technological research. The new material originates with new opportunities to review old problems as well as stance new ones. The recent discovery of graphene, a single layer of graphite brought such an exciting period of research and technology interest.¹ Graphene is a two-dimensional building block of covalently bonded sp² hybridized carbon and allotropes of other carbon-based materials. It can be rolled into one-dimensional nanotubes, stacked into three-dimensional graphite, or wrapped into zero-dimensional fullerene. The interesting electronic, optical, mechanical and thermal properties have offered the great prosperity of graphene for several applications. The variety of technological application based on graphene requires producing the graphene on a large scale.

The large number of methods have been proposed to produce graphene in high quality. The present approaches fail to scale up the graphene production in large scale. Micromechanical cleavage is attuned for high-quality graphene sheet, but the low productivity of this method makes it incompatible for large-scale usage. The

methods for exfoliation of graphene in solution process can produce large-scale materials and adopt the process for breaking the stacking force between the graphitic layers. This can be carried out mainly by two major approaches: sonication of graphite in solvents and chemical functionalization (e.g., graphene oxide). The sonication exfoliation method aids the experimental preparation for graphene sheet remarkably. However, the continuous sonication is stranded to give the higher yield of graphene and excessive sonication can lead to the destruction of the graphene.²⁻⁵ Chemical functionalization of graphite (e.g. graphite oxide) is an efficient approach to the bulk production of graphene sheet at low cost. But, the process requires the contribution of hazardous strong oxidizing (e.g. H₂SO₄/KMnO₄) and reduction reagents.⁶

The simple planetary ball milling can employed for non-destructive and large-scale production of graphene sheets in recent years.⁷ However, Difficult to exfoliate the graphite through dry ball milling due to the plate like the structure of graphite layers. Wet ball milling of graphite with organic solvents is the possible way for the preparation of good quality graphene, but the exfoliation efficiency needs to be improved.⁸ Production of graphene by ball milling of graphite with dry ice or melamine was demonstrated.⁹ The introduction of oxalic acid as a reductant for preparation of high-quality graphene from graphene oxide (GO), also demonstrated.¹⁰ The CVD process offers a large scale graphene production but the usage of toxic chemicals may generates hazardous waste with poisonous gases. This method is complicated and consume high production cost.¹¹ Accordingly, the necessity to develop a simple approach that should be environment friendly and agree for scalable graphene production at low cost.

^a CSIR-Institute of Minerals and Materials Technology, Bhubaneswar-751 013, India

^b Department of Electrical and Computer Engineering, Pusan National University,

^c San 30, Jangjeong-Dong, Gumjeong-Ku, Busan-609 735, South Korea.

^d Electronic Supplementary Information (ESI) available: Dual-Drive Planetary Ball milling System, Energy Dispersive X-ray spectra of synthesized graphene sheets, Milling time Vs lattice strain and Crystallite size, Critical Speed with respect to Gyro and Jar speed calculation. See DOI: 10.1039/x0xx00000x

In this work, we employed the shear-force dominated milling of graphite with oxalic acid for scaled up of graphene production (50g per jar) at extremely low cost. The shear force and mill assisting agent plays a vital role in non-destructive graphene production in ball milling process. The dynamics of shear force milling measured by the percentage of critical speed that depends on the gyrating and jar speed in dual drive ball milling system. The shear dominated milling optimized by the rotation speed of the vials & shaft holding the vials, Ball to powder weight ratio, milling time, Type and size of grinding medium and milling container. The critical speed is the key factor in deciding the shear and impact energy of the balls-to-powder. The critical speed is estimated using equation 1 and tabulated in supporting information.

The dual drive ball milling can produce 50g of graphene powder (in a single jar) and 200g of graphene powder in a unique milling cycle. The main advantage of dual drive ball milling is the simple process, cost effectiveness, and large scale production compared to other graphene preparation techniques. The inevitable inclusion of metal impurities into the surface of graphene sheets from the balls, energy gradient between the balls to powder, and inhomogeneous crystalline (size and shape) formation with impurities and grain boundaries are the disadvantage of this method. This work is mainly focused to develop the shear force dominated ball milling for scalable and non-destructive graphene production and to investigate the quality of the graphene by the complementary characterization techniques along with utilization of Pd nanostructure for electrocatalytic for the formic acid oxidation process.

2. Experimental

2.1 Raw materials

Graphite flakes (Product no. 332461, Sigma-Aldrich) and Oxalic acid dihydrate (ACS reagent, Product no.247537, Sigma-Aldrich) were used.

2.2 Synthesis of Graphene

In a typical procedure, 50g of graphite flakes and 80g of oxalic acid (OA) were placed into stainless steel jar (2500 ml volume) containing 10 mm diameter of stainless steel balls used as grinding medium. The utilization of low diameter stainless steel balls are due to increase the impact and shear energy of the ball to powder and make a low dimensional interaction with graphite layers. Initially, the Dual-drive ball milling was executed at three different critical speeds (40%, 70%, and 98%). But the critical speed of 40% offers an efficient exfoliation with less defects than 70% and 98%. Accordingly, the optimized critical speed of 40% is adopted for the graphite exfoliation by shear force ball milling. The milling was carried out up to 20 h and rest time was one hour per cycle. Then, the milled graphite was treated with 1M Hydrochloric acid (HCl) to acidify the carboxylates and to remove the Iron impurities from milling jar in the milled graphite. Then, the mixture was washed with distilled water for several times until the pH becomes neutral. The mixture was filtered and subjected to the heat treatment at 600°C under an argon atmosphere for an appropriate time interval. Finally, as-prepared graphene was stored for prior use.

2.3 Synthesis of Graphene-Pd Nanocomposites

A 3 mg of as-prepared graphene powder was taken in 30 ml of DMF and dispersed by sonication for 10 min and stirred further for 30 minutes. Then 0.6 ml of 50 mM PdCl₂ was added to the graphene dispersed DMF solution and allowed to mix under stirring condition. Then 0.6 ml of NaBH₄ (50 mM) was added dropwise and allowed

the entire mixture under stirring condition for 30 minutes. After, the sample was separated by centrifuge and washed properly to remove the DMF and unreacted species. The sample was dried and kept in a desiccator for prior use.

2.4 Characterization

The X-ray diffraction (XRD) patterns of ball milled graphite were collected using a PANalytical's X-ray diffractometer equipped with the Ni-filtered CuK α radiation source ($\lambda=1.54\text{\AA}$). The radiation source has operated at generator voltage 40 kV and a current of 40 mA. The XRD data was recorded in the range of 20–40(2 θ), in a step scan mode with a step width 0.05 and a time of 1sec per each step. Transmission electron microscope (TEM) images were obtained using an FEI Tecnai G2 TEM operating at 200 kV. The specimens were prepared by dropping 2 μL of colloidal solution onto carbon-coated copper grids. The X-ray photoelectron spectroscopy (XPS) analysis was carried out on a Specs (Germany) X-ray photoelectron spectrometer. The high-resolution spectra were recorded using 20 eV pass energy with Mg K α 12,586 eV radiation.

2.5 Electrochemical measurements

The electrochemical analyzes were performed using a two-compartment three-electrode cell with a glassy carbon working electrode (area 0.07 cm²), a Platinum wire as auxiliary electrode and Ag/AgCl (3M KCl) as a reference electrode. Cyclic voltammogram were recorded using a computer-controlled CHI660C electrochemical analyzer (CHI, USA). The as-synthesized materials were dispersed over a glassy carbon electrode with Nafion and dried prior to electrochemical experiments.

3. Results and discussion

3.1 Mechanism of graphite exfoliation by shear force dominated ball milling

The shear force dominated ball milling of graphite with oxalic acid was carried out under optimized critical speeds (40%, 70%, and 98%). In this process, the graphene sheet can be exfoliated layer by layer from the graphite. The weak Vander Waals interaction between the graphitic layers may resist the graphene exfoliation. The high energy ball milling typically offers the impact and shear forces between the balls to powder. The impact force can overcome the Vander Waals forces of graphite layers to deliver uncontrolled exfoliation in a destructive way (Micromechanical cleavage using scotch tape).¹² The shear force delivers an essential and controlled energy to diminish the Vander Waals interaction and encourage the relative motion between the graphitic layers for ease exfoliation of graphene sheets. The mill assisting agent (oxalic acid) provides a great support for non-destructive exfoliation. The dehydrogenation of oxalic acid (reducing agent) possess a strong oxygen free radicals that confined the carbonyl group in the edges of graphite. The additional fragmentation effect may cause during the exfoliation process when the absence of optimization of critical speed. This effect may result to the inevitable inclusion of impurities and structural defects. The schematic representation of the mechanism is shown in Figure 1.

3.2 Structural analysis of graphene sheets

The XRD patterns of post-milled graphite/oxalic acid at different milling hours are shown in Figure 2. The presence of (002) diffraction peak confirm the milled graphite is in the ordered crystal structure.¹³⁻¹⁵ According to the JCPDS (03-065-6212), the diffraction pattern of the graphite and milled graphite is dominated by strong (0 0 2) plane at 26.6°.

The continuous decrease in the intensity of the (002) peak at 10 h and 20 h of experiments indicates the reduction of size and thickness of graphite. This observation supports the exfoliation of graphene from bulk graphite. After 20 h of post-milling, few peaks were left. The heat treatment diminishes the impurity peaks and increase the intensity of 002 planes that might be the agglomeration of graphene sheets. With increasing the milling time, the (002) peak was shifted towards lower angles, suggesting the widening of d_{002} spacing. The crystalline size gradually decreases with increasing strain according to increase in milling time, depicted in figure 2.

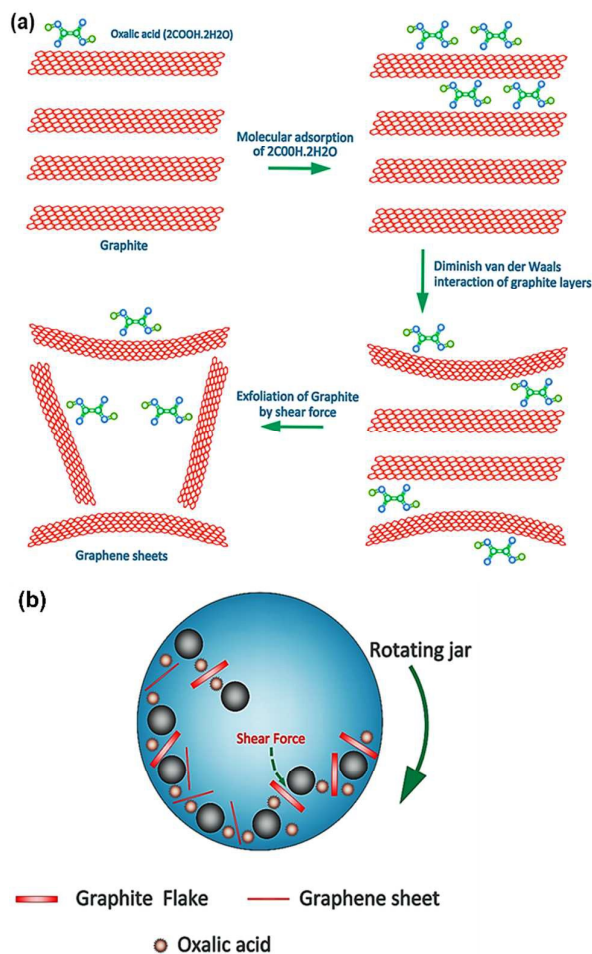


Figure 1. a) Mechanism of graphite exfoliation by shear-force ball milling b) Schematic representation of ball milling of graphite with oxalic acid.

3.3 Raman Spectroscopy of Graphene sheets

Raman spectroscopy is a powerful non-destructive tool to further estimate the thickness and purity of the as-prepared graphene. Raman spectra of graphite, post-milled graphite at 20 h, annealed at 600°C and comparison of graphene preparation at different critical speed is presented in figure 3(a) and (b). For graphite, G band (1570 cm^{-1}), 2D band (2708 cm^{-1}) and a weak D band have been observed. The post-milled graphite with oxalic acid for 20 h showed a strong D band at 1350 cm^{-1} that correspond to the breathing modes of sp^2 carbon atoms.

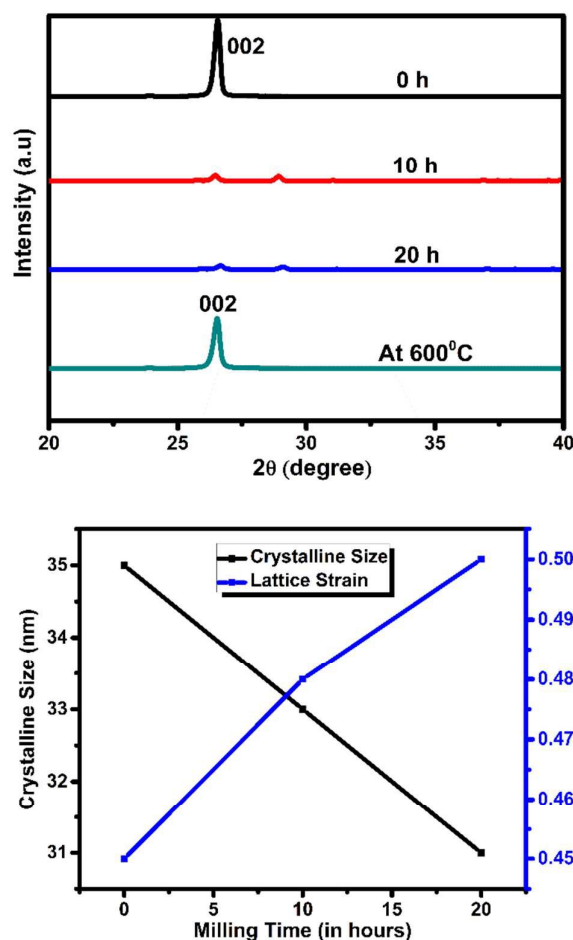


Figure 2. XRD patterns of graphite and post milled graphite/oxalic acid for different milling periods as 0 h, 10 h, and 20h at 40% critical speed. The crystalline size and strain calculation with respect to the milling time.

The G peak is the result of first-order scattering of the E_{2g} mode of graphite and is related to the in-plane vibration of sp^2 hybridized carbon-carbon bonds that arises at 1580 cm^{-1} . The 2D band arises around 2700 cm^{-1} due to second phonon vibrations of sp^2 carbon atoms.¹⁶ In this case, the 2D peak is quite broad and D' peak appears around the shoulder of G peak at 1585 cm^{-1} which suggested that the characteristic of bilayer graphene sheets. This observation is well-matched with the report.⁵ The intensity ratio I_D/I_G value of isolated graphene at 20 h is ~ 0.57 , much lower than the value of chemically derived graphene by reduction of graphite oxide.

As expected, the D peak from the inside of an isolated graphene sheet has almost disappeared by the heat treatment at 600°C for 5 min. The I_D/I_G value of annealed graphene has given ~ 0.09 that indicates the heat treatment increased the quality of the material. The intensity ratio I_{2D}/I_G is calculated to be ~ 0.41 that specified the thickness of graphene sheet.¹⁷⁻¹⁹ Critical speed is the important parameter in ball milling technique to get high quality graphene sheet. In this work, we attempted to perform the milling process of graphite with oxalic acid at different critical speeds of 40%, 70% and 98% for 20 hours.

Figure 3b revealed that 40% critical speed shows better results than 98% and 70% critical speed in dual-drive ball mill system. It can be deduced here that the slow speed can efficiently exfoliate the graphene sheet from graphite with lower defects. The 98% and 70% critical speed cause fast grinding than 40% critical speed. At higher critical speed, the exfoliation has occurred efficiently but the defects are quite high. The purity of the material is calculated from the intensity ratio I_D/I_G is ~ 0.53 for 40%, ~ 0.59 for 70% and ~ 0.62 for 98% critical speed respectively (Table 3). The number of layers in graphene sheet at different critical speed was determined from the I_{2D}/I_G ratio presented in Table 3.

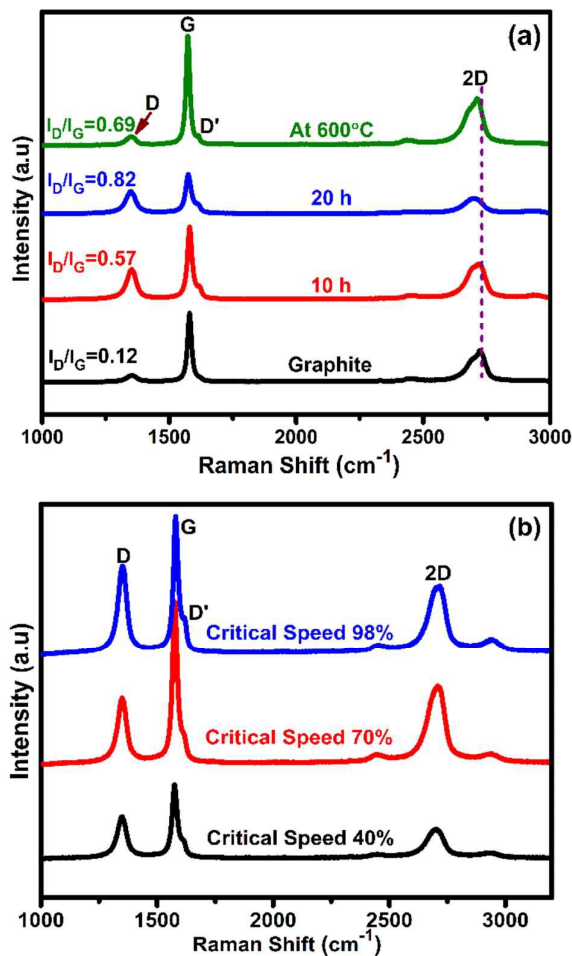


Figure 3. Raman spectra of ball-milled graphite/oxalic acid a) 10 hours, 20 hours and annealed at 600°C b) at different critical speed for 20 hours.

3.4 Transmission Electron Microscopy (TEM) of Graphene sheets

The TEM measurements were carried out to determine the degree of exfoliation and the morphology of the graphene sheet.^{20, 21} The Selected Area (Electron) Diffraction (SAD) patterns were recorded to identify the crystal structures and the measure lattice parameters. The TEM images of graphite and as-prepared graphene sheet and their corresponding SAD patterns are shown in Figure 4. The pure graphite flakes slightly transparent under electron beam and irregular sheets are stacked. The SAD pattern of graphite flake clearly confirmed the polycrystalline nature of the graphite (Figure 4b). Figure 4(c) specified that the exfoliated graphene sheet were

quite transparent under the electron beam, suggesting that the very small thickness of the graphene sheet. The single and bilayer graphene sheets were clearly visualized in TEM image.

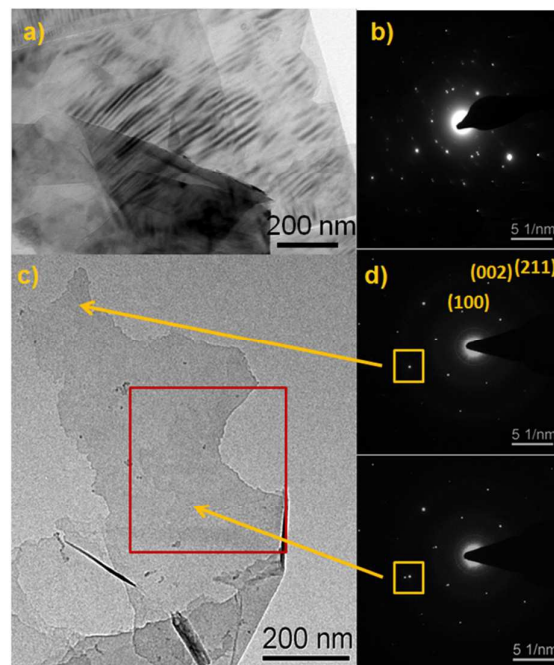


Figure 4. TEM images of (a) graphite, (b) corresponding SAD pattern (c) representative graphene sheets with the SAD patterns for single and bilayer graphene sheets.

The corresponding SAD pattern confirmed the single layer graphene represented from the six point crystal system. Also, two set of six point crystal systems that are closely arranged is observed. This validates that the sample might be having bilayer graphene sheets. This validates that the oxalic acid assisted exfoliation of graphite by shear milling is non-destructive and also providing a great platform for the mass production of high quality graphene sheets.²²

X-Ray Photoelectron Spectroscopy (XPS) is a quantitative surface analysis technique which used to identify the chemical composition and binding states of as-prepared graphene sheet. Figure 5 shows the C 1s core-level spectra of both graphite and graphene with the prominent C 1s peak appeared at 284.7 eV, assigned to the sp^2 vibrational carbon atoms. The similar pattern of graphite and graphene has revealing that the intrinsic structure of graphite remains largely intact during the post-milling treatment. It suggested that the shear dominated ball milling doesn't affect the intrinsic structure of graphene sheet. The weak peak at 290.6 eV that corresponds to π - π transitions of graphitic carbon which appeared only in graphite. The component at 287.5 eV has been usually attributed to C=O (carbonyl and carboxylic) groups of both graphite and graphene. The size of graphite reduced while milling, confirmed from the change in peak intensity, binding energy positions and atomic concentration of graphite and graphene. Figure 6 represents the surface binding states of O 1s for graphite and graphene.

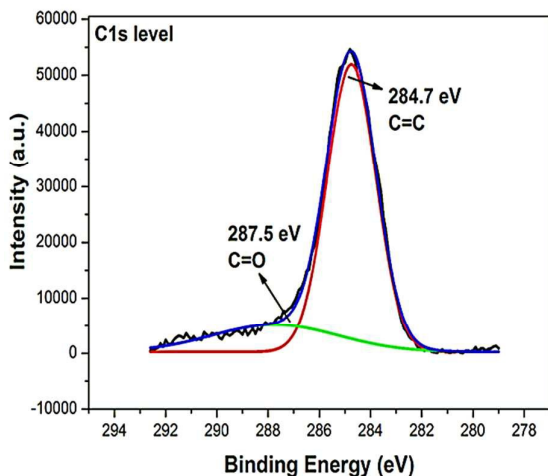
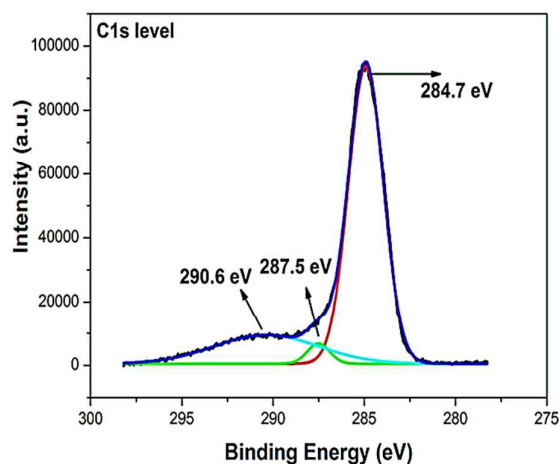


Figure 5. C 1s binding states of graphite and graphene

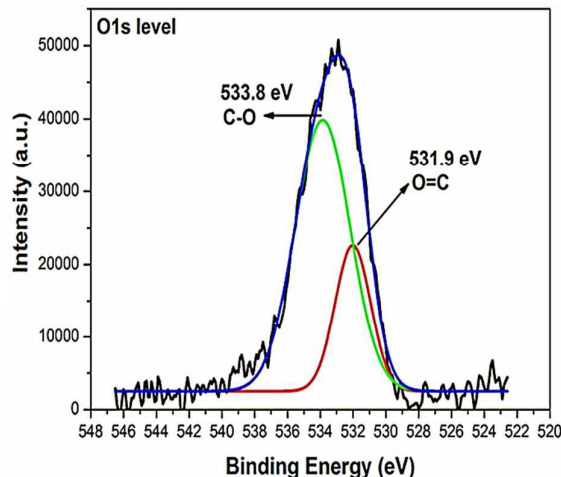
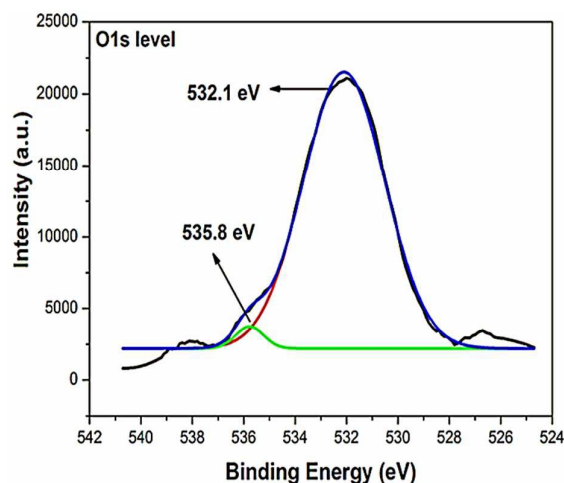


Figure 6. O 1s binding states of graphite and graphene

Besides a trace amount of O 1s peak arising at 532.1 eV and 531.9 eV for graphite and graphene, assigned to C=O binding state. The peak located at 535.8 eV in graphite, might be physically adsorbed water or oxygen from the addition of oxalic acid.²³

Electrochemical studies of Graphene-Palladium Nanocomposites

The graphene supported Pd nanocomposites synthesized by a facile one step approach. The Pd precursor was dispersed with as-synthesized graphene sheet and reduced to form the Pd nanostructures on graphene surface. The TEM measurements were carried out to investigate the morphology of Pd nanostructures grown on graphene surface and presented in figure 7. Here, we choose formic acid as the typical molecule to study the electrocatalytic activity of graphene-palladium nanocomposite. Interestingly, the tiny Pd nanostructures are well dispersed on graphene support.

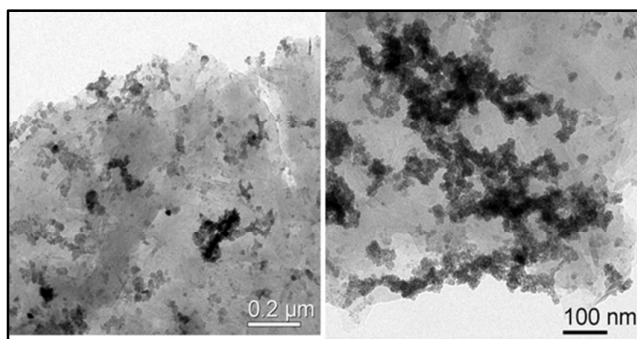


Figure 7. TEM image of graphene supported Pd nanostructures.

The Pd nanostructures got agglomerated on some part of graphene surface during the drying process. The electrochemical oxidation of formic acid is a very much useful process in the energy sector due to its potential energy related applications. Various hybrid catalysts have been prepared to enhance formic acid oxidation. It has been documented that the Pt-based catalyst provided outstanding catalytic performance towards formic acid oxidation.

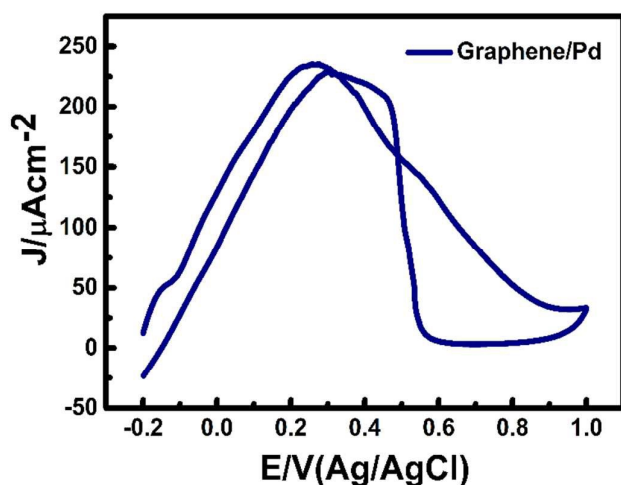


Figure 8. Cyclic voltammogram for oxidation of formic acid (0.25M) in 0.1M HClO₄ acid

However, the Pt surface intensely adsorbs the CO species created as a reaction intermediate and causes the surface poisoning. The Pd-based catalyst has been explored to be efficient and possess superior performances for fuel cell applications because it is highly resistance towards CO poisoning. Therefore, the electrocatalytic performance of as-synthesized graphene-Pd nanocomposites was explored towards formic acid oxidation (Figure 8). A well-defined inverted V-shaped voltammogram with prominent oxidation peak at 0.263 V was observed on graphene-Pd nanocomposites modified electrode. The onset potential for formic acid oxidation is -0.1 V. The oxidation current has been normalized to the electro-active surface area of the graphene assisted Pd nanostructures. This surface area was determined from the coulombic charge reduction of Pd oxide according to the reported value of 424 $\mu\text{C}/\text{cm}^2$.^{21,24} Though the onset potentials of formic acid oxidation calculated -0.15 V and -0.49 V for graphene-Pd composites obtained by sonication exfoliation method,²⁵ modified Hummer method²⁶ respectively. The graphene based Pd nanocomposites prepared by ball milling show comparable onset potential -0.1 V and oxidation peak at 0.263 V. Our efforts are underway to improve the quality graphene-Pd nanocomposite to deduce the effect of the substrate in electrocatalytic activity towards formic acid for fuel cell interest.

Conclusions

We employed a simple shear force dominated planetary ball milling for preparing graphene in large scale (200g per cycle) with less structural defects. The optimized critical speed (40%) can efficiently exfoliate the graphene sheet from graphite, evidenced by Raman spectroscopic analysis. The onset potential for formic acid oxidation is -0.1 V with prominent oxidation peak at 0.263 V. The graphene based Pd nanostructures show improved catalytic activity for formic acid oxidation which suggest that the Pd nanostructure well dispersed on graphene surface. This is the first time the graphene prepared by ball milling has utilized with Pd nanostructures for electrocatalytic applications. This work is an initial approach for scale up production of graphene that will promote further towards the fuel cell applications.

Acknowledgements

This work was supported and funded by Council of Scientific and Industrial Research (CSIR) governed by the Indian government (No.ESC-401). The first author would like to thank Prof. D. Mangalaraj, Dr. C. Viswanathan, and Dr. N. Ponpandian, Department of Nanoscience and Technology, Bharathiar University, for their extraordinary support and encouragement throughout this work. The first author thank to Mr. R. Parthipan, for his assistance in artwork.

Notes and references

1. A. K. Geim and K. S. Novoselov, *Nature materials*, 2007, **6**, 183-191.
2. T. Lin, J. Chen, H. Bi, D. Wan, F. Huang, X. Xie and M. Jiang, *J. Mater. Chem.A*, 2013, **1**, 500-504.
3. L. Liu, Z. Xiong, D. Hu, G. Wu and P. Chen, *Chem. Commun.*, 2013, **49**, 7890-7892.
4. J. C. Meyer, A. K. Geim, M. Katsnelson, K. Novoselov, T. Booth and S. Roth, *Nature*, 2007, **446**, 60-63.
5. W. Zhao, M. Fang, F. Wu, H. Wu, L. Wang and G. Chen, *J. Mater. Chem.*, 2010, **20**, 5817-5819.
6. V. León, M. Quintana, M. A. Herrero, J. L. Fierro, A. de la Hoz, M. Prato and E. Vazquez, *Chemical Communications*, 2011, **47**, 10936-10938.
7. X. Yue, H. Wang, S. Wang, F. Zhang and R. Zhang, *Journal of Alloys and Compounds*, 2010, **505**, 286-290.
8. S. Park and R. S. Ruoff, *Nature nanotechnology*, 2009, **4**, 217-224.
9. M. Choucair, P. Thordarson and J. A. Stride, *Nature Nanotechnology*, 2009, **4**, 30-33.
10. P. Song, X. Zhang, M. Sun, X. Cui and Y. Lin, *Rsc Advances*, 2012, **2**, 1168-1173.
11. Y. Zhang, L. Zhang and C. Zhou, *Acc. Chem. Res.*, 2013, **46**, 2329-2339.
12. M. Yi and Z. Shen, *J. Mater. Chem.A*, 2015, **3**, 11700-11715.
13. M. J. Allen, V. C. Tung and R. B. Kaner, *Chem. Rev.*, 2009, **110**, 132-145.
14. S. Gadipelli and Z. X. Guo, *Progress in Materials Science*, 2015, **69**, 1-60.
15. V. Singh, D. Joung, L. Zhai, S. Das, S. I. Khondaker and S. Seal, *Progress in Materials Science*, 2011, **56**, 1178-1271.
16. S. Lee, K. Lee and Z. Zhong, *Nano letters*, 2010, **10**, 4702-4707.
17. A. C. Ferrari, *Solid State Commun.*, 2007, **143**, 47-57.
18. D. Palmer, 1967.
19. S. Stankovich, R. D. Piner, S. T. Nguyen and R. S. Ruoff, *Carbon*, 2006, **44**, 3342-3347.
20. O. Akhavan, *ACS nano*, 2010, **4**, 4174-4180.
21. S. C. Sahu, A. K. Samantara, B. Satpati, S. Bhattacharjee and B. K. Jena, *Nanoscale*, 2013, **5**, 11265-11274.
22. D. Li and R. B. Kaner, *Nat Nanotechnol*, 2008, **3**, 101.
23. J. Zhang, B. Guo, Y. Yang, W. Shen, Y. Wang, X. Zhou, H. Wu and S. Guo, *Carbon*, 2015, **84**, 469-478.
24. I.-Y. Jeon, H.-J. Choi, S.-M. Jung, J.-M. Seo, M.-J. Kim, L. Dai and J.-B. Baek, *J. Am. Chem. Soc.*, 2012, **135**, 1386-1393.
25. S. Yang, J. Dong, Z. Yao, C. Shen, X. Shi, Y. Tian, S. Lin and X. Zhang, *Scientific reports*, 2014, **4**.
26. L. Gao, W. Yue, S. Tao and L. Fan, *Langmuir*, 2013, **29**, 957-964.